A level set method for the construction of anisotropic boundary-conforming Voronoi regions and Delaunay triangulations

Ümit Keskin and Joaquim Peiró

Department of Aeronautics, Imperial College London,
South Kensington Campus, London SW7 2AZ, United Kingdom
e-mail: u.keskin09@imperial.ac.uk, j.peiro@imperial.ac.uk

Summary. We interpret a Voronoi region as the shape achieved by a crystal that grows from a seed and stops growing when it reaches either the domain boundary or another crystal. Using this analogy we devise a method for generating *anisotropic boundary-conforming* Voronoi regions and their dual Delaunay triangulation for a set of points. The method simulates the propagation of crystals as evolving fronts modelled by a level set method. The generation of anisotropic Voronoi regions is achieved by re-interpreting the user-specificied Riemmanian metric in terms of the propagation speed normal to the boundary of the crystal.

Key words: Voronoi diagrams; Delaunay triangulation; level set method; crystal growth; Riemannian metric; anisotropic meshes

1 Introduction

Anisotropy in the generation of Voronoi regions is desirable when one tries to generate meshes where elements are required to be stretched along certain directions such as in aerofoil boundary layers and wakes. The Riemannian metric field required to generate anisotropic mesh elements with spatial variations in size and shape is often incorporated in practice through the use of local tranformations [3], but such methods do not guarantee the validity of a dual Delaunay triangulation. Some recent theoretical progress in that direction is reported in [2, 5, 4].

Here we propose a technique based on crystal growth with a propagation speed dictated by the Riemannian metric field that permits a straightforward generation of anisotropic Voronoi regions that conform to a prescribed boundary and their dual anisotropic Delaunay triangulation with stretched triangles, which is one of the most problematic aspects of mesh generation using a Voronoi-based approach.

2 Formulation

The growth of the crystals from an initial set of S seeds is modelled by a combined formulation of those proposed in [9, 7]. The front of each crystal, denoted by the index s, is assimilated to a constant value of a function $\varphi^s(x, y, t)$ that evolves according to the equation

$$\frac{\partial \varphi^s}{\partial t} + \beta^s F^s \left|\nabla \varphi^s\right| = 0 \quad s = 1, \ldots, S. \tag{1}$$

Here F^s is the speed of propagation in the direction normal to the crystal, φ^s, β^s is a sensor to detect the collision of the crystal with other crystals or the boundary. A modified version of the sensor proposed by [7] that allows for an arbitrary number of crystals to meet at a point is used to detect these collisions. The treatment of the collision with the boundary as if it was a crystal leads to isolated regions. To remedy this problem, we impose a dry contact of the crystal with the boundary, i.e. we require the normal component of the velocity of the crystal at the boundary to be zero.

We introduce anisotropy via a user-specified spatial distribution of the metric tensor, $\mathbb{M}(x, y)$, e.g. [3, 2], and a level set speed function, $F^s(x, y)$, given by

$$F^s \propto \sqrt{\mathbf{N}^{s^T}\, \mathbb{M}\, \mathbf{N}^s} \tag{2}$$

where $\mathbf{N}^s$ is the direction of the normal to boundary of the crystal, generated from seed s, evaluated at (x, y).

The governing equations (1) are solved using the explicit finite-differences discretization proposed in [9]. An example of growth of a set of crystals using a user-specified metric field is shown in Fig. 1. The metric field is depicted in Fig. 1(a) where the axes of the ellipses are inversely proportional to the eigenvalues of the metric tensor. The speed function at a point is calculated as a weighted average of the values of the speed function for each specified metric tensor. The evolution of the crystals, shown in Fig. 1(b), illustrates the consistency between the present method and the specified metric field.

3 Examples of application

The first example deals with the generation of boundary-conforming Voronoi regions for a computational domain which is the interior region to two curves that exhibit convex and concave segments. Fig.2(a) and 2(b) show the metric field and the Voronoi regions generated from 17 seeds, respectively. This example illustrates the ability of the method to generate Voronoi regions that conform to boundaries of arbitrary topology. Using a 200×200 mesh, it took approximately 770 seconds (for a 2.13 GHz processor) to reach the steady-state crystal configuration shown in Fig.2.

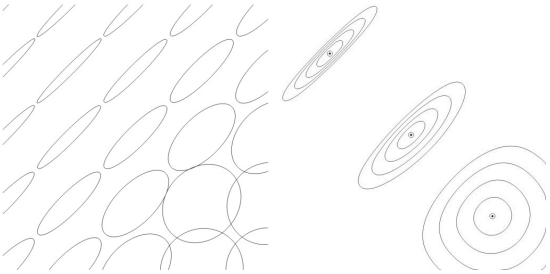

(a) (b)

Fig. 1. Crystal growth governed by a spatially-varying metric field: (a) ellipses represent the metric field; and (b) growth of the crystals.

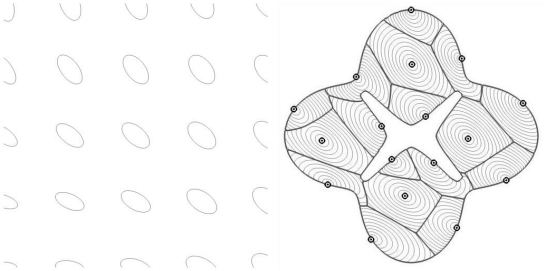

(a) (b)

Fig. 2. A complex domain: (a) prescribed anisotropic metric field; (b) boundary-conforming Voronoi partition.

In the second example we consider the region around a symmetric aerofoil with a distribution of 130 seeds located uniformly away from the aerofoil and clustered in the normal direction near the aerofoil surface and wake. We consider isotropic and anisotropic metric fields shown in Figs. 3(a) and 3(f), respectively. In the anisotropic case, the metric tensor at a point on the aerofoil surface is aligned with the tangent at that point. The Voronoi partitions obtained with these metric fields are shown in Figs. 3(c) and 3(d) for the isotropic and anisotropic cases, respectively. The dual Delaunay triangulations for these were constructed by joining two colliding seeds with a line segment. The resulting isotropic and anisotropic Delaunay triangulations are shown in Figs. 3(e) and 3(f), respectively. Both Delaunay triangulations are valid, but looking more closely at the mesh in the region in the wake near the trailing edge, we notice the mesh obtained with an isotropic mesh field, shown in Fig. 3(g) and which corresponds to a conventional Delaunay triangulation, exhibits triangles stretched in the direction perpendicular to the wake. This is an undesirable but well-documented, e.g. [1], feature of using an isotropic metric field and clustered points in the normal direction. The usual remedy

here is to modify the mesh via side swapping, but then the result is no longer a Delaunay triangulation. On the other hand, the mesh generated using the anisotropic metric field in Fig. 3(h) does not have such problems and the triangles are stretched along the right direction.

4 Conclusions

We have presented a level set method for generating Voronoi regions, and their dual Delaunay triangulations, that complies with a user-specified metric field through the specification of an appropriate speed function. The method permits a straightforward treatment of the interfaces between regions and, more importantly, addresses in a natural manner two major issues in Delaunay-based mesh generators: the generation of highly-stretched Voronoi regions and the conformity to non-convex realistic boundaries.

The cost of computations depends on the number of seeds and the size of the rectangular mesh, which is determined by the minimum distance between the seeds. The mesh size also determines the number of timesteps required to converge to the final Voronoi partition due to the CFL stability restriction of the explicit time integration used. The method can be readily implemented in 3D but efficiency will be an issue. However, performance improvements can be achieved using the narrow band [8] or the fast marching [6] methods that have not been incorporated in the current implementation.

References

1. T. J. Barth. Aspects of unstructured grids and finite-volume solvers for the Euler and Navier-Stokes equations. VKI lecture notes 1994-05, 1995.
2. Q. Du and D. Wang. Anisotropic centroidal Voronoi tessellations and their applications. *SIAM J. Sci. Comp.*, 26(3):737–761, 2005.
3. P.-L. George and H. Borouchaki. *Delaunay Triangulation and Meshing: Application to Finite Elements*. Hermes, 1998.
4. C. Wormser J.D. Boissonnat and M. Yvinec. Anisotropic diagrams: Labelle-Shewchuk approach revisited. *Theoretical Computer Science*, (408):163–173, 2008.
5. F. Labelle and J. R. Shewchuk. Anisotropic Voronoi diagrams and guaranteed-quality anisotropic mesh generation. In *SoCG'03*, pages 191–200, 2003.
6. G. Peyre and L. D. Cohen. Geodesic methods for shape and surface processing. *Advances in Computational Vision and Medical Image Processing: Methods and Applications*, pages 29–56, 2009.
7. G. Russo and P. Smereka. A level set method for the evolution of faceted crystals. *SIAM J. Sci. Comp.*, 21(6):2073–2095, 2000.
8. J. A. Sethian. *Level Set Methods and Fast Marching Methods*. Cambridge University Press, second edition, 1999.
9. J. A. Sethian and J. Strain. Crystal growth and dendritic solidification. *Journal of Computational Physics*, 98:231–253, 1992.

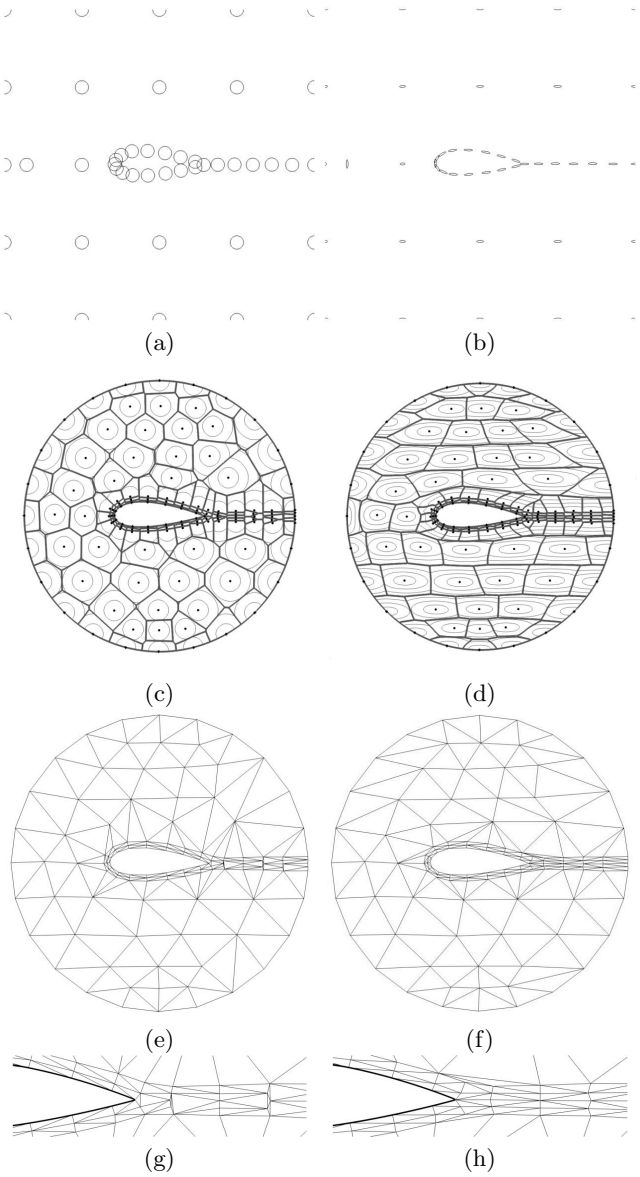

Fig. 3. Comparison for a domain around a symmetric aerofoil: The distribution of the isotropic (a) and anisotropic (b) metric fields; corresponding Voronoi partitions (c) and (d); the complete Delaunay triangulations (e,f); and enlargement near the wake of the aerofoil (g,h). Notice how the introduction of anisotropy in the metric field aligns the triangles with the wake as required.